Design and implementation of a predictive current controller applied to regulate a battery bank's power flow connected to a DC microgrid

Pedro H. Peters Barbosa[1], João P. Peters Barbosa[1], Pedro M. Almeida[1], Rodolfo L. Valle[1,2]
[1]Federal University of Juiz de Fora, Juiz de Fora - MG, Brazil
[2]Federal Center of Technological Education of Minas Gerais, Leopoldina, Brazil
e-mail: pedro.peters@engenharia.ufjf.br

***Abstract* - This paper presents steps of the design and implementation of a digital predictive controller applied to the regulation of the flow of current in a battery bank. The set converter/battery is the energy storage system management of a DC microgrid that will be connected to the grid. Whenever the grid is disconnected from the DC microgrid, it becomes necessary a fast response from the bus's voltage control. Due to its fast response and simple implementation, predictive current controllers are attractive to this sort of application. The control algorithm was implemented in a low cost TIVA EK-TM4C123GXL platform from Texas Instruments and experimental results will be obtained by a 15 kW converter.**

***Keywords* – Predictive current control, Synchronous Buck, Bidirectional DC-DC Converter.**

I. INTRODUCTION

Having centralized electric power system (EPS) located at great distances from consumer centers, besides increasing the conduction losses, saturates prematurely the transmission line due to the constant energy demand. Furthermore, small consumer centers far from EPS may not be supplied [1, 2].

With the intent of solving such problems, new theories and propositions have been investigated and discussed, for instance, the distributed generations system (DGS). In this way, renewable sources have strong appeal due to reduced greenhouse gases emission. This sources, when connected to the grid, increase the energy offer next to the load centers, postponing the construction of new transmission lines and enhancing the energy quality mainly at moments of heavy loads [3–5].

In this sense, smart-grid researches have similar goals to DGS, such as introduction of renewable sources, increase the reliability and security of power grids, as well as load management [6].

The Brazilian government has approved a resolution that defines micro and mini distributed generation [7] and, in 2016, Brazil had an increase of 440% on micro and mini generation over the previous year. That reveals the potential of this kind of energy generation in the country [7].

However, most of the renewable sources currently installed in Brazil generate currents and voltages in DC [5]. Due to the fact that the instants of generation and consumption are not the same, it is necessary to use energy storage systems, such as batteries. Computers, notebooks, cellphones and TVs have AC-DC converters that reduce their efficiencies. Thus, the idea of a DC micro-grid becomes attractive due to less conversion stages, less cable energy losses caused by skin effect and, not being necessary synchronization or unbalanced phase like in an AC micro-grid. Besides that, the losses can be reduced from 10% to 32% in a DC micro-grid [8–13].

Figure 1 shows the proposed DC microgrid diagram block. AC and DC loads are connected to the DC bus, which is composed by a capacitor bank. There are also renewable sources like photovoltaic panels and wind turbines tracking the maximum power point and supplying the DC bus. Despite the multiple power sources, this sources provide an intermittent flow of energy, therefore making necessary a battery power bank.

In case the power generated is larger than the power consumed, the excess energy is stored in a battery, if the battery's state of charge is low. However, when the consumed power is larger than the generated power, the batteries must provide power to the DC bus in islanding moments. A bidirectional DC-DC converter interfaces the DC bus and the battery bank, which can inject or drain energy from the DC bus.

Whenever there is islanding, the converter/battery set has to quickly inject current in the DC bus, in order to prevent the bus's voltage from sagging.

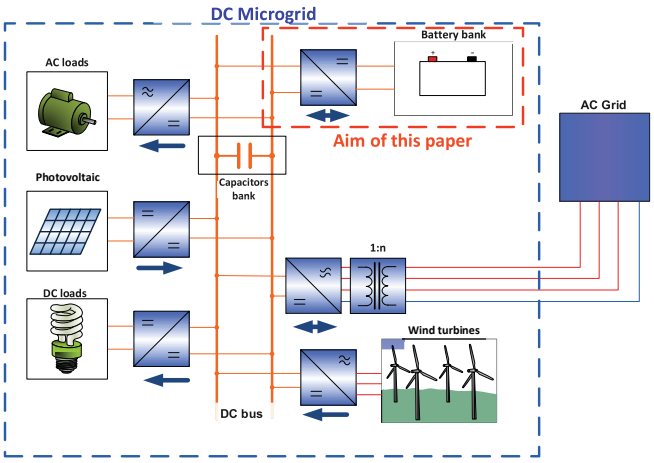

Fig. 1. : DC microgrid and detail of the aimed paper.

Predictive controllers have been used successfully as means of controlling DC-DC converters, since they posses some striking traits as the fast response and simple implementation

978-1-5090-6248-5/17/$31.00 ©

in microprocessed systems.

This paper presents the design and implementation steps of a digital predictive controller applied to a DC-DC converter used as interface between the DC bus and the battery bank. A synchronous buck converter is used to control the level and direction of the battery bank's current, as shown in detail of the Figure 1.

II. THE SYNCHRONOUS DC-DC CONVERTER

Considering the DC bus voltage being inferior to that of the battery bank's, it becomes necessary to implement a stage of DC-DC conversion. The buck was made to operate synchronously, meaning that instead of using a switch and a diode the converter uses two switches, rendering it more efficient and with smoother transitions between operation modes.

The bidirectional capability of this converter permits the charge (boost stage) or the discharge (buck stage) of the battery bank, controlling the current and voltages.

Figure 2 shows the schematic diagram of a bidirectional DC/DC converter. In this figure, V_{bus} and V_{BB} are the terminal voltage of DC bus and battery pack, respectively, and i_L is the inductor current. The PWM pattern of S_1 and S_2 is complementary, so that when switch S_1 is closed, S_2 is open and vice-versa.

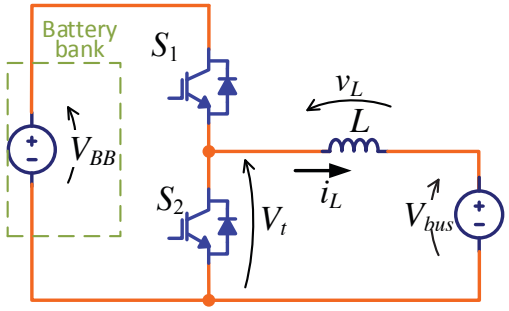

Fig. 2. : Synchronous buck converter.

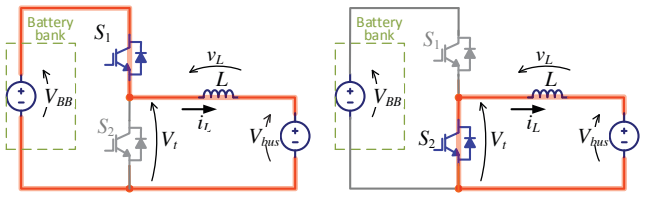

Fig. 3. : Stages of converter: (a) S_1 on and S_2 off, (b) S_1 off and S_2 on.

Figure 3 (a) and (b) show the two stages of the synchronous buck converter. When S_1 is on, the terminal voltage is given by $V_t = V_{BB}$; and when S_2 is on, the terminal voltage is $V_t = 0\,V$.

A. Digital Predictive Controller

The principle of predictive controller applied to this converter is very simple. Figure 4 shows the predictive current controller waveforms. The voltage control (v_c) when compared with the triangular carrier (v_{tri}) defines the duty cycle ($d[k]$) to drive the power semiconductor S_1 and consequently S_2, creating the PWM signals. The inductor current and the reference is given by i_L and i_L^*, respectively. The voltages V_{bus} and V_{BB} and the current i_L are sampled every time that the triangular carrier assumes its minimum value.

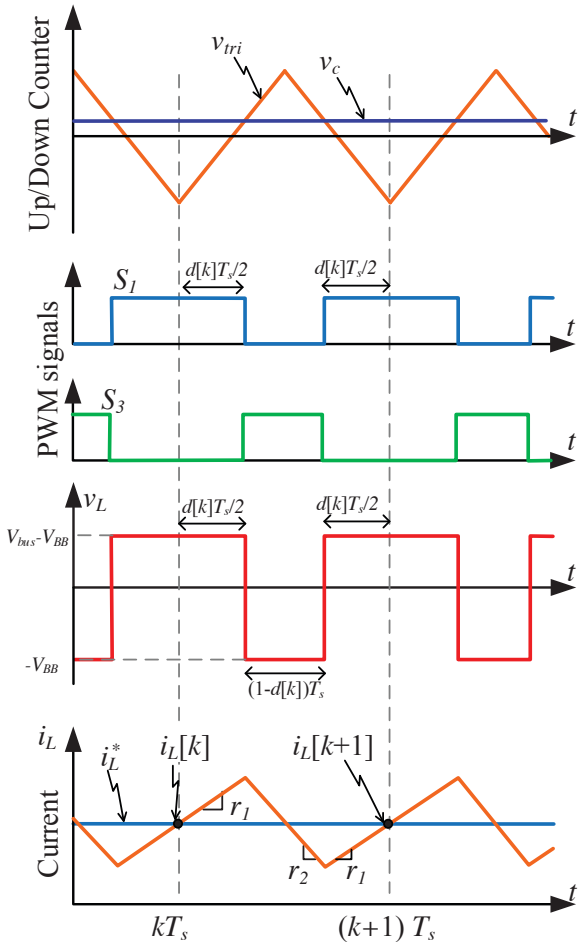

Fig. 4. : Predictive current controller waveforms: (a) Up/Down counter, (b) PWM signals, (c) inductor voltage and (d) inductor current and reference

Considering that $i_L > 0$, we can write a expression to the inductor current in the next sample [14]:

$$i_L[k+1] = i_L[k] + r_1 d[k] T_s + r_2 (1 - d[k]) T_s \qquad (1)$$

where r_1 and r_2 are the inductor current rise and fall rates, respectively, which is given by:

$$r_1 = \frac{V_{BB} - V_{bus}}{L} \qquad (2)$$

$$r_2 = \frac{-V_{bus}}{L} \qquad (3)$$

Substituting (2) and (3) into (1) and isolating $d[k]$:

$$d[k] = \frac{Lf_s}{V_{BB}}(i_L^* - i_L[k]) + \frac{V_{bus}}{V_{BB}}, \quad (4)$$

where $i_L^* = i_L[k+1]$ is the reference inductor current that must be tracked by the converter and $f_s = 1/T_s$ is the sample frequency of the digital predictive controller.

From (4) it is possible to determine the desired duty cycle, based on the instant current obtained in the inductor, the reference current and respective voltages V_{BB} and V_{bus}. Taking into account the computational effort and time necessary to realize the mathematical operations, the following law is also applied in two consecutive sample times:

$$i_L[k+2] = i_L[k+1] + r_1 d[k+1]T_s + r_2(1-d[k+1])T_s \quad (5)$$

Substituting (1) in (5) and, in this result, substituting (2) and (3) and isolating $d[k+1]$:

$$d[k+1] = \frac{Lf_s}{V_{BB}}(i_L^* - i_L[k]) - d[k] + \frac{2V_{bus}}{V_{BB}}, \quad (6)$$

where $d[k+1]$ is the duty cycle that has been updated in $[k+1]T_s$ instant and $i_L^* = i_L[k+2]$ is the new current reference.

Analyzing (6) it is possible to obtain the duty cycle that will be applied in the instant $[k+1]T_s$, in a way that the current in the inductor in the instant $[k+2]T_s$ acquires the reference current value. This way the reference current will be tracked with two sample cycles of delay. Sampling the current i_L in the minimum value of the triangular carrier allows the acquisition of the current's average value without the need of passive or digital filters

III. Simulation Results

The control system of the current in the battery was implemented in the simulation software PSIM, with the intent of verifying the strategy of control proposed. The parameters were adjusted to $L = 2\ mH$, $f_s = 10\ kHz$, $V_{bus} = 12\ V$, and $V_{BB} = 48\ V$ was replaced by a $C = 0.1\ F$ capacitor to allow a better understanding of the voltage output of the battery, being the predictive controller simulated using (6).

Figure 5 (a) shows the current waveform in the inductor. When t = 0.01 s, a step variation from 1 A to 2 A is applied to the reference current amplitude, which will be tracked by the converter. In the t = 0.015 s instant, another step variation is made to the reference current amplitude, this time from 2 A to 0 A. Lastly, when t = 0.02 s, another step variation happens, this time from 0 A to -2 A.

In Fig. 5 (a) the three steps in current simulate different stages of charge in the battery. The first step in the reference current amplitude represents the discharging stage of the battery during islanding, whereas the second represents the discharged state and the third represents the charging stage after the islanding period ends.

In order to clarify the variations of voltage output from the battery bank during the simulation steps, the voltage values over the $C = 0.1\ F$ capacitor were measured and are as Fig.5 (b) shows.

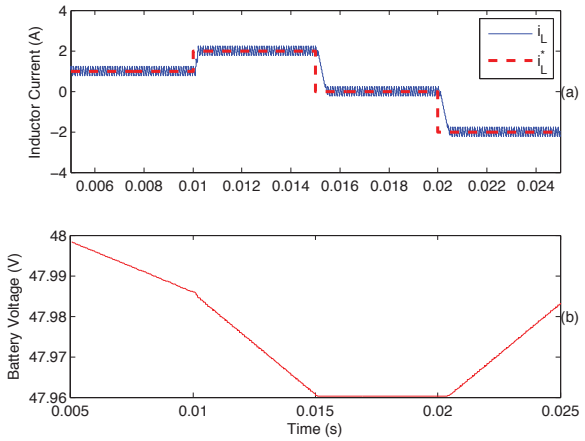

Fig. 5. : Current in the inductor and voltage in the battery

The digital model used in the simulation can also be used to investigate the sturdiness of the controller when dealing with sudden variations of parameters. Figure 7 shows the predictive control response to the scenarios where it is implemented in converters with different inductances. For simulation purposes, the different converter inductances were chosen as $L_1 = 2.4\ mH$ and $L_2 = 1.6\ mH$, therefore being 20% higher or lower when compared to the original inductance L.

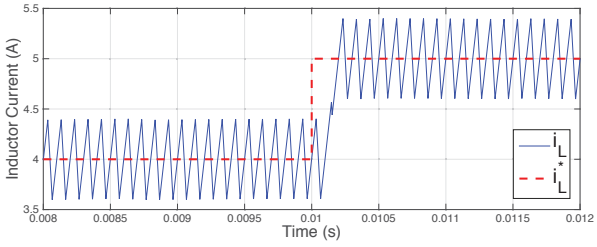

Fig. 6. : Current step response of predictive controller.

IV. Experimental results

A 15 kW DC-DC synchronous buck converter was used to validate the simulation results as well as the predictive controller design methodology presented in this work. The bidirectional converter uses two Semikron SK45 GB 063 IGBT modules connected in parallel. The digital current controller was implemented using the TIVA EK-TM4C123GXL platform from Texas Instruments. Fig. 8 shows the picture of the experimental setup. Table I shows the parameter setup used to obtain the experimental results.

TABLE I: Experimental setup parameters

Parameter	Value
Battery Pack Voltage (V_{BB})	48 V
Bus Voltage (V_{bus})	12 V
Inductance (L)	2 mH
Switching Frequency (f_s)	20 kHz

Fig. 9 shows the experimental results of the predictive current controller given by (6). A step current reference is applied

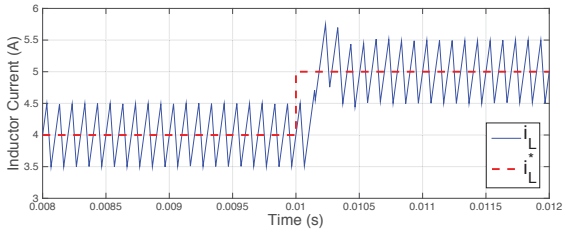

(a)

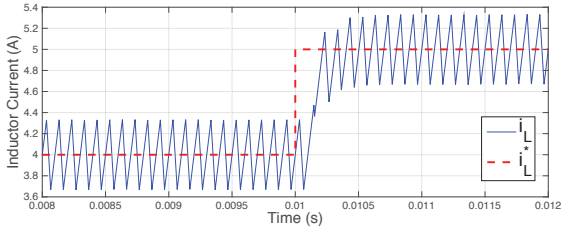

(b)

Fig. 7. : Current step response in converters with: (a) higher inductance(L_1), (b) lower inductance(L_2).

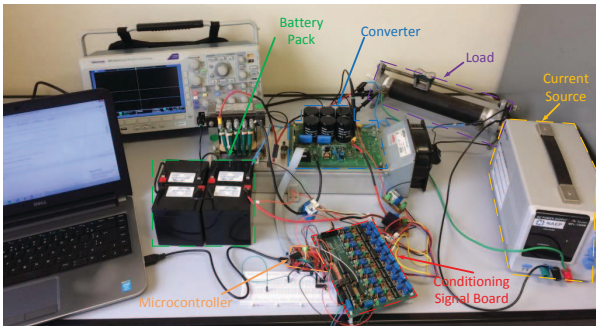

Fig. 8. : Experimental prototype.

from 1 A to 2 A. It is possible to see that after as short tracking period, the output current in the inductor rapidly reaches the desired value of i_L^* similarly to the simulation.

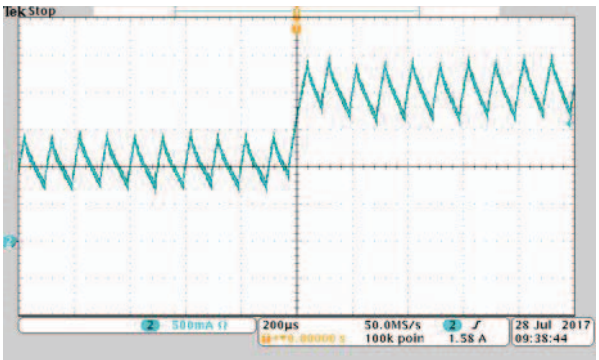

Fig. 9. : Current step response in experimental prototype.

Fig. 10 shows the experimental results of the predictive control response to the scenarios where variations in L parameter are considered, as can be made in the simulations of Fig. 7. Likewise to the simulation, the different parameter inductances controller were chosen as $L_1 = 2.4\ mH$ and $L_2 = 1.6\ mH$, Fig. 10(a) and (b), respectively, therefore being 20% higher or lower when compared to the original inductance L. The current of the compensated system presents a stable behavior even variations of 20% in L parameter.

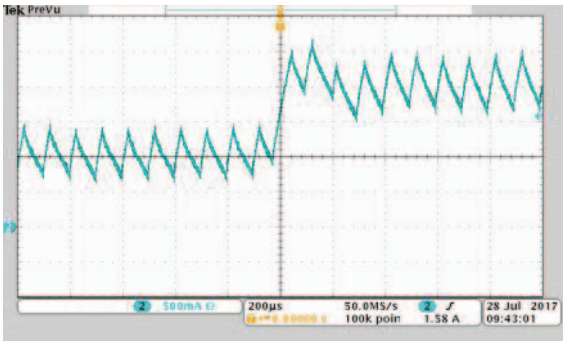

(a)

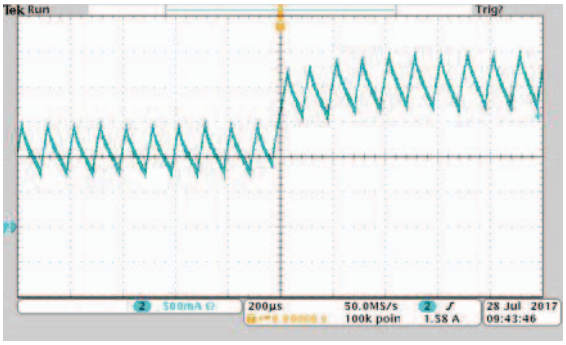

(b)

Fig. 10. : Current step response in converters with: (a) higher inductance($L_1 = 2.4\ mH$), (b) lower inductance($L_2 = 1.6\ mH$).

Fig. 11 shows the experimental setup used to verify the bus voltage controller. A current source (i_{gen}) represents the renewable sources generation. A voltage controller was designed to regulate the bus voltage. Additionally to the current control, a *PI* voltage controller was implemented in order to regulate the bus voltage. The *PI* gains are given by $k_p = 0.4\ V/A$ and $k_i = 150\ V/A.s$

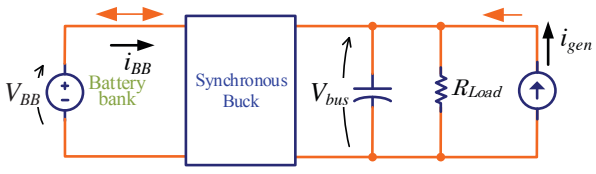

Fig. 11. : Block diagram of the experimental setup to the voltage controller.

In Fig. 12, the experimental results of the battery voltage, DC bus voltage and inductor current for the control of the DC bus voltage are shown, considering the case of islanding. Initially, the generated power is equal to the consumed power. In $t = 4\ s$, there is a reduction in the energy supply from the

renewable sources and the inductor current assumes positive value, in other words, the battery supplies energy to the microgrid DC bus. Approximately in $t = 16\ s$, the generated power is equal to the consumed power by the load and the average current is zero. When $t = 26\ s$ the generated power is bigger than the consumed one, and the average current assumes negative value while the battery is being charged. When $t = 35\ s$ there is an abrupt variation in the generated power and the current assumes once again positive value. It is observed that even under variations in the generated power, the DC bus voltage remains constant, demonstrating a good response by the voltage controller.

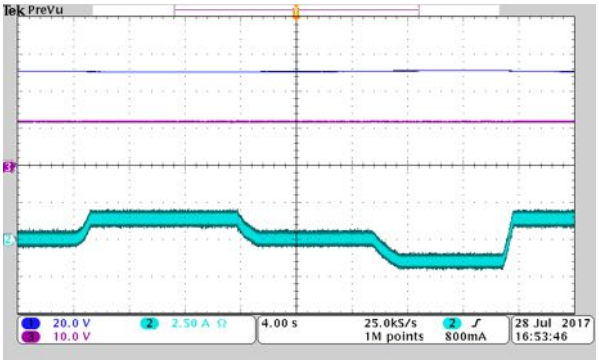

Fig. 12. : Voltage controller: battery pack voltage (Channel 1), bus voltage (Channel 3) and inductor current (Channel 2).

V. CONCLUSION

This paper presented the steps design of a current predictive controller applied to a battery bank. The battery/converter set was used in a DC microgrid to control the voltage DC bus during the islanding periods. The current control law was obtained based on the model, demonstrating its simplicity and easy implementation. The simulation and experimental results shows the feasibility of the used algorithm control system. The current behavior was investigated considering parameter variations. Due to the low computer burden the algorithm can be implemented in a low cost platform.

ACKNOWLEDGEMENT

The authors would like to express their gratitude to UFJF, CEFET-MG, FAPEMIG, CAPES and CNPq for the financial support and scholarships.

REFERENCES

[1] Pedro Machado de Almeida. *Contribuições ao estudo de conexão de sistemas fotovoltaicos rede elétrica sem filtros passivos: projeto de controladores digitais para redução do conteúdo harmônico*. Ph.d. thesis, 2013.

[2] Rodrigo Arruda Felcio Ferreira. *Controle de microrredes CC baseado em droop adaptativo de tensão simulação em tempo real com control-hardware-in-loop*. Ph.d. thesis, 2013.

[3] Leandro Borges Pedro M. Almeida Pedro S. Almeida Rodolfo L. Valle Rodrigo Ferreira André Ferreira Pedro Barbosa Henrique Braga Márcio Rodrigues, André Moura. Proposal of a hybrid dc/ac microgrid integrating renewable energy sources into a smart building. PCIM, 2012.

[4] Filipe Caixeiro Mattos, Vinicius Sobreira Lacerda, Rodolfo Lacerda Valle, Andre Augusto Ferreira, Pedro Gomes Barbosa, and Henrique Antonio Carvalho Braga. Contribution to the study of a single-phase and single stage photovoltaic system. *IEEE Latin America Transactions*, 13(5):1265–1271, 2015.

[5] ANEEL. Cadernos temáticos aneel micro e minigeração distribuda sistema de compensação de energia elétrica., 2016.

[6] Paul Savage, Robert R Nordhaus, and Sean P Jamieson. Dc microgrids: Benefits and barriers. *From Silos to Systems: Issues in Clean Energy and Climate Change*, pages 51–66, 2010.

[7] ANEEL. Nota técnica n 0056/2017-srd/aneel, maio de 2017.

[8] D. Chen and L. Xu. Autonomous dc voltage control of a dc microgrid with multiple slack terminals. *IEEE Transactions on Power Systems*, 27(4):1897–1905, Nov 2012.

[9] R. S. Balog, W. W. Weaver, and P. T. Krein. The load as an energy asset in a distributed dc smartgrid architecture. *IEEE Transactions on Smart Grid*, 3(1):253–260, March 2012.

[10] M. Kumar, S. N. Singh, and S. C. Srivastava. Design and control of smart dc microgrid for integration of renewable energy sources. In *2012 IEEE Power and Energy Society General Meeting*, pages 1–7, July 2012.

[11] C. M. Lai, C. T. Pan, and M. C. Cheng. High-efficiency modular high step-up interleaved boost converter for dc-microgrid applications. *IEEE Transactions on Industry Applications*, 48(1):161–171, Jan 2012.

[12] A. A. A. Radwan and Y. A. R. I. Mohamed. Assessment and mitigation of interaction dynamics in hybrid ac/dc distribution generation systems. *IEEE Transactions on Smart Grid*, 3(3):1382–1393, Sept 2012.

[13] M. Kumar, S. C. Srivastava, and S. N. Singh. Dynamic performance analysis of dc microgrid with a proposed control strategy for single-phase vcvsi. In *2014 IEEE PES T D Conference and Exposition*, pages 1–6, April 2014.

[14] Jingquan Chen, A. Prodic, R. W. Erickson, and D. Maksimovic. Predictive digital current programmed control. *IEEE Transactions on Power Electronics*, 18(1):411–419, Jan 2003.